

## Electrocatalytic activity of electrochemically deposited Zr-Ce-Y/Ni and Co/Zr-Ce-Y/Ni oxide systems during evolution of hydrogen and oxygen

A. S. Tsanev<sup>1</sup>, P. Ts. Iliev<sup>2</sup>, K. M. Petrov<sup>2</sup>, P. K. Stefanov<sup>1</sup>, D. S. Stoychev<sup>3\*</sup>

<sup>1</sup> Institute of General and Inorganic Chemistry, Bulgarian Academy of Sciences,  
Acad. G. Bonchev St., Block 11, 1113 Sofia, Bulgaria

<sup>2</sup> Institute of Electrochemistry and Energy Systems, Bulgarian Academy of Sciences,  
Acad. G. Bonchev St., Block 10, 1113 Sofia, Bulgaria

<sup>3</sup> Acad. R. Kaishev Institute of Physical Chemistry, Bulgarian Academy of Sciences,  
Acad. G. Bonchev St., Block 11, 1113 Sofia, Bulgaria

Received January 28, 2008, Revised February 25, 2008

The possibilities of obtaining the ternary oxide system  $\text{CeO}_2\text{-ZrO}_2\text{-Y}_2\text{O}_3$  on Ni foam in an electrochemical way were investigated. Cobalt oxide was additionally deposited on the ternary system. The catalytic effect with respect to oxygen and hydrogen evolution in alkaline electrolyte was investigated. Electrolysis regimes and compositions permitting variation of the Ce:Zr:Y ratio within large limits were established. The structure, morphology and distribution of the elements in the layers being formed were defined. The system  $\text{CoO/CeO}_2\text{-ZrO}_2\text{-Y}_2\text{O}_3/\text{Ni}$  was shown to catalyze the evolution of oxygen, decreasing the reaction potential by about 200 mV.

**Key words:** electrodeposition, electrocatalytic activity, electrodes, CoO.

### INTRODUCTION

The specific properties of ceria, permitting it to act as an oxygen pump through the redox pair  $\text{Ce}^{3+}/\text{Ce}^{4+}$ , determine its extremely wide application in various catalytically active systems. Its high capacity with respect to accumulation/donation of oxygen (OSC) contributes to its high catalytic activity. In addition,  $\text{CeO}_2$  in the role of “support” of various catalysts (usually noble metals) contributes to the increase and stabilization of their dispersion [1]. Thanks to these properties,  $\text{CeO}_2$  participates as a main component in the so-called “three-way” catalysts (TWC) for purification of waste gases from internal combustion engines. An important disadvantage of ceria, however, is its insufficient thermal stability. At high temperatures, a significant reactivation of the redox pair is observed due to sintering of the latter [2]. The incorporation of zirconium ions into the lattice of ceria leads to its thermal stabilization but at low temperatures OSC is not high enough to control the harmful gases. For that reason, a system with a high OSC and a high catalytic activity at low temperatures was to be looked for [3].

It is known that IV group oxides containing low-valency cations and having a fluorite structure are good ion conductors and are often used as electrochemical oxygen pumps. Yttrium oxide, for instance,

has a lower valency (+3) and ensures additional increase in oxygen vacancies of the crystal lattice. This leads to an increase of OSC [4, 5]. In addition, the mechanical strength of the system is enhanced [6].

All the above facts have led to focusing the attention of a number of authors on the system Zr-Ce and finding more fields of applications for it. In addition to the TWC catalysts there are also: a catalyst for reforming ethanol and obtaining hydrogen [7]; a catalyst for oxidation of methane [8], electrode materials in Magnetohydrodynamic (MHD) energy conversion units [9]; Solid Oxide Fuel Cells (SOFC) (due to their mixed conductivity) [10] and toughened ceramics [11], etc.

Investigations on the ternary system Zr-Ce-Y are not many in number. Most of them deal with its application in SOFC [12, 13] or as a catalyst in TWC [14, 15]. Among the few authors paying attention to its application as electrode for electro-catalysis, one should mention Y. Xiong *et al.* [16], but they have no direct investigations on the catalytic properties.

Even less are the studies on the electrochemically obtained Zr-Ce-Y oxide systems. Taking into account that when compared to the other conventional methods, the electrochemical preparation of thin films has a series of advantages such as low deposition temperatures, high frequency and definite chemical composition of the deposited layers, precise control of the film thickness and a good adhesion to the substrate [17, 18], the layers

\* To whom all correspondence should be sent:  
E-mail: stoychev@ipchp.ipc.bas.bg

obtained in this way are a promising alternative. It can be assumed that the electrochemical preparation would lead to definite structural changes and peculiarities which could also affect the change in catalytic properties of the system Zr-Ce-Y [19–20]. In cases when the system is used as a support, this way of preparation would also influence the catalytic capacity of the complex “metal substrate/Zr-Ce-Y layer/active phase”.

The purpose of the present paper was the electrochemical preparation and characterization of thin Zr-Ce-Y layers on a Ni foam. The second purpose was to test this system separately and in combination with  $\text{CoO}_{\text{ox}}$  deposited on it as an active phase for oxygen and hydrogen evolution in alkaline electrolytes.

## EXPERIMENTAL

Samples of 1x1 cm area and thickness of 50  $\mu\text{m}$  cut from a standard sheet of stainless steel OC 4004, were used for the experiments. This steel had the following composition (%): Cr (18.00), Al (5.00), C (0.02) and Fe (balance). Prior to the electrochemical deposition of the Ce-Zr-Y oxides layer, the samples were subjected to standard procedures of degreasing with organic solvents, Vienna lime and hot alkaline solutions [21]. After careful washing with distilled water and drying at 100°C for 10 min the samples were immersed for 60 min in an alcohol electrolyte containing: 80 g/l  $\text{CeCl}_3$ , 10 g/l  $\text{ZrCl}_4$  and 35 g/l  $\text{YCl}_3$ . Electrolysis was performed in potentiostatic regime at a forming voltage of 10–20 V. The chemical states and composition of the layers were investigated by XPS analysis using a VG Escalab Mk II spectrometer (England) with an Al  $K_{\alpha}$  excitation source (1486.6 eV) and a total instrumental resolution of  $\sim 1$  eV, under a base pressure of  $1 \times 10^{-8}$  Pa. The O 1s, Ce 3d, Zr 3d and Y 3d photoelectron lines were calibrated to the C 1s line. The spectra were recovered after 2 min  $\text{Ar}^+$  bombardment of the samples. The surface composition of the mixed oxide layers was determined from the ratio of the corresponding peak intensities, corrected with the photoionization cross-sections [22].

The surface morphology of the samples was examined by a JEOL JSM 6390 scanning electron microscope (Japan) equipped with an ultrahigh resolution scanning system in a regime of secondary electron image (SEI). The accelerating voltage was 25 kV,  $I \sim 65$  mA and vacuume  $10^{-6}$  Torr.

The structure and phase composition of the electrochemically deposited films were identified by X-ray diffraction (XRD) analysis with a Philips diffractometer using  $\text{Cu } K_{\alpha}$  radiation. The acquisi-

tion conditions were  $2\Theta$  from 20 to 80°.

The same Ce-Zr-Y oxide layers were also deposited on substrates of nickel “foam” with a round cross-section ( $\Phi$  24 mm). Layers of  $\text{CoO}$  were additionally deposited on this system (Ni/Ce-Zr-Y oxide) to obtain the system  $\text{CoO/CeO}_2\text{-ZrO}_2\text{-Y}_2\text{O}_3/\text{Ni}$ .

The samples obtained were used for preparing gas diffusion electrodes (GDE) as follows: a gas-layer of hydrophobized (with 45% Teflon) acetylene soot was pressed to a tablet at  $P = 300$   $\text{kg/cm}^2$  and  $T = 300^\circ\text{C}$ . A  $\text{CeO}_2\text{-ZrO}_2\text{-Y}_2\text{O}_3$  or  $\text{CoO/CeO}_2\text{-ZrO}_2\text{-Y}_2\text{O}_3$  layer was pressed on the tablet at  $P = 150$   $\text{kg/cm}^2$  and  $T = 300^\circ\text{C}$ . The same GDE were used for measuring the electrochemical characteristics with respect to the reactions of evolution and reduction of oxygen. An electrochemical cell with a special construction permitting gas (air or oxygen) introduction to the gas-layer was used. The counter-electrode was a nickel sponge, the reference electrode –  $\text{HgO/Hg}$ , and the working electrolyte – 20%  $\text{KOH}$ . Steady-state voltamper curves were obtained in a galvanostatic regime by a Solartron 1286 potentiostat-galvanostat.

## RESULTS AND DISCUSSION

### SEM, EDS and XRD investigations

The results from SEM studies on the structure and surface morphology of electrochemically deposited  $\text{ZrO}_2\text{-CeO}_2\text{-YO}_{1.5}$  layers with a thickness of about 1  $\mu\text{m}$  are presented in Fig. 1. They are cracked but have a good adhesion to the substrate (Figs. 1a and 1b).

The difference in the size of the agglomerates and cracks-forming zones A and B and the quantitative changes in their chemical composition were determined for characteristic zones and points. Their typical morphology is shown in Figs. 1c and 1d.

The EDS analyses in zones A show an enhanced concentration of  $\text{CeO}_2$  in the layer (the tables below the images 1d and 1e) while in zones B the chemical composition (the Zr/Ce/Y ratio, respectively) is close to that characteristic of  $\text{ZrO}_2\text{-CeO}_2\text{-YO}_{1.5}$  layers obtained by different conventional methods [3]. On the basis of these results one may assume that the reduction of the cerium-containing complexes is predominating with respect to zirconium and yttrium-containing complexes. It begins and proceeds mainly on definite active sites of the substrate and not uniformly on the whole surface. It was also established that the crystallite size in the separate agglomerates forming the layers depended on crystallites with sizes of about 20 nm (Fig. 1e).

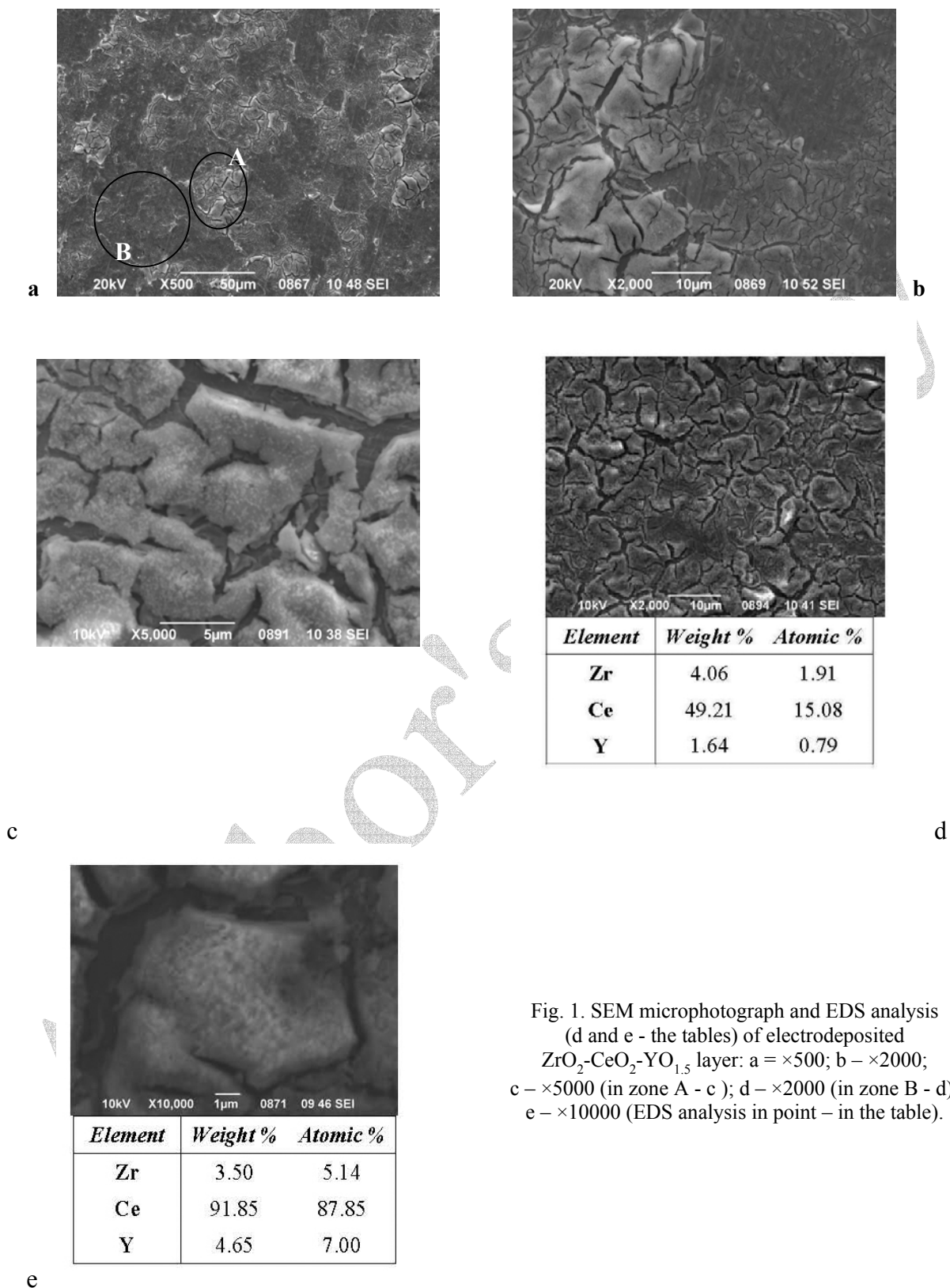


Fig. 1. SEM microphotograph and EDS analysis (d and e - the tables) of electrodeposited  $ZrO_2-CeO_2-YO_{1.5}$  layer: a -  $\times 500$ ; b -  $\times 2000$ ; c -  $\times 5000$  (in zone A - c); d -  $\times 2000$  (in zone B - d); e -  $\times 10000$  (EDS analysis in point - in the table).

The registered specific distribution of ceria leading to strongly cracked light zones A (Fig. 1c) determines a mean value of the Ce/Zr ratio in the layers of about 17, which varies from about 26 in A light zones to about 12 in dark B zones. The oxygen concentration established in A zones is much higher than in B zones, which is in a good agreement with the data on high OSC of ceria [23].

The EDS analyses in a map regime also show an uniform distribution of zirconia and yttria, contrary to the case of ceria (Fig. 2).

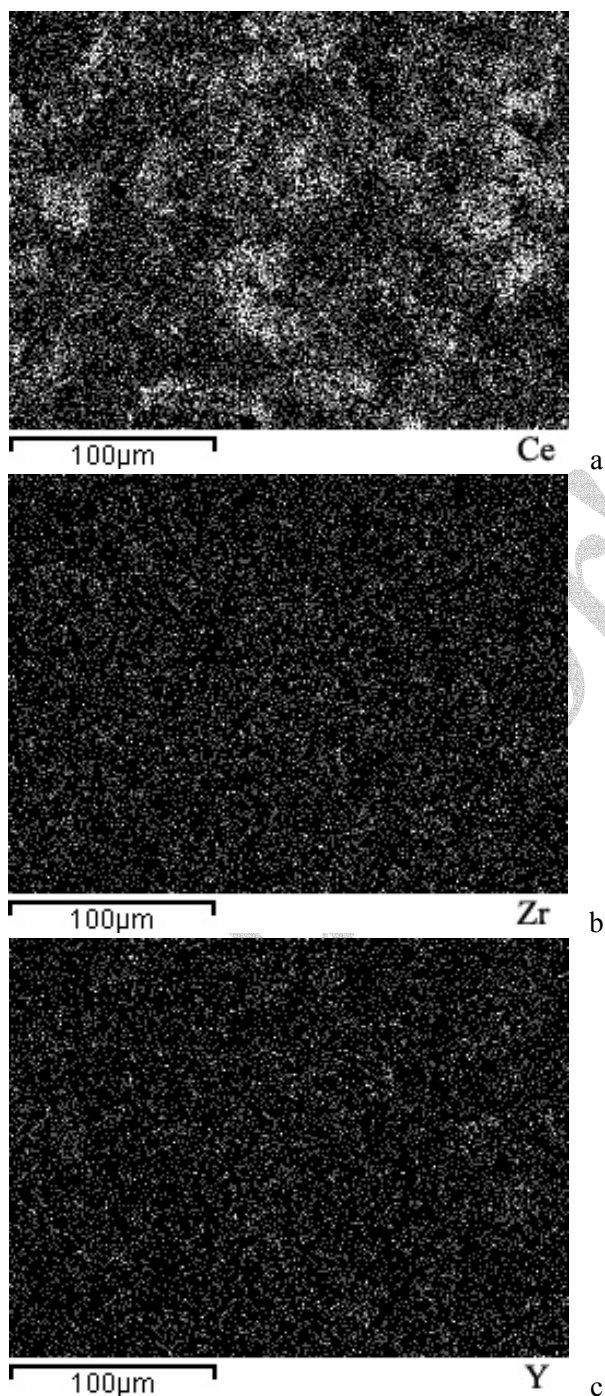


Fig. 2. EDS analysis of the distribution of Ce (a), Zr (b) and Y (c) in  $ZrO_2-CeO_2-YO_{1.5}$  layers - in map regime.

This result permits to assume that zirconia and yttria are incorporated into the lattice of ceria, which is in agreement with the XRD data (Fig. 3). The XRD analyses are made on layers deposited upon stainless steel because the highly rough surface of nickel foam does not permit precise X-ray studies. Both as deposited and annealed samples have been investigated.

According to literature data [19], ceria crystallizes in a lattice with fluorite structure (space group  $Fm\bar{3}m$ ) whereas zirconia is monoclinic (space group  $P2_1/c$ ). The difference in cationic radii of ceria (0.097 nm) and zirconia (0.084 nm) presupposes their restricted mutual solubility. As a result, only two thermodynamically stable phases (tetragonal and cubic) have been found, with high and low zirconia contents, respectively. Two metastable tetragonal phases,  $t'$  and  $t''$ , have also been observed [24].

Figure 3 shows that the reflections of the polar figure of the freshly deposited sample are characterized by a large width that corresponds to phases with small particles. This would obviously result in a large “working” surface of the deposited phase. With a view to more precise indexing of the peaks, the samples were subjected to XRD study after the annealing. Then the peaks at 28.6 and 33.1, typical of cubic cerium, were registered [25]. No visible peaks for separate zirconium and cerium phases were registered. There was only a slight shift of the cerium peaks to larger angles, which can be ascribed [26] to incorporation of zirconium into the lattice of cerium and formation of a solid solution. We are of the opinion that this shift is due to the smaller cationic radius of Zr (IV) as compared to Ce(IV) and, hence, to the decrease in lattice parameter. It is also important to note that the peaks are symmetric, which eliminates the presence of polymorphism in the deposited sample.

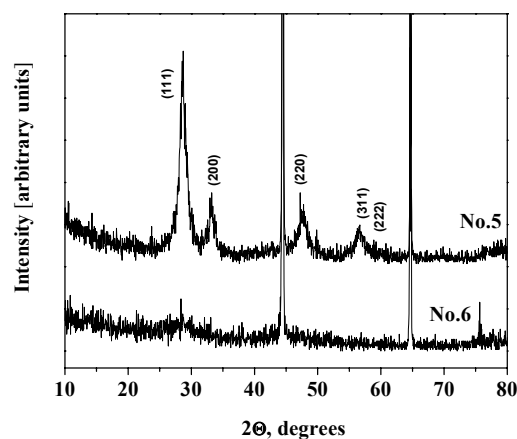


Fig. 3. XRD patterns of as deposited (No. 6) and annealed (No. 5)  $ZrO_2-CeO_2-YO_{1.5}$  layers.

The structural peculiarities found with the  $ZrO_2$ - $CeO_2$ - $YO_{1.5}$  layers and their specific affinity to oxygen, i.e. the enhanced electronic conductance [27], were the reason to test them as supports of CoO active phase.

Figure 4 shows a SEM microphotograph of a  $ZrO_2$ - $CeO_2$ - $YO_{1.5}$  layer with a thin Co oxide layer deposited on it. Evidently, it forms pyramidal agglomerates situated uniformly on a  $ZrO_2$ - $CeO_2$ - $YO_{1.5}$  layer. The XPS analyses of such systems showed (Fig. 5) that the electrodeposited CoO layer practically screened the  $ZrO_2$ - $CeO_2$ - $YO_{1.5}$  sublayer. On the basis of the place of the cobalt peak it may be concluded that the main amount of cobalt has been electrodeposited as  $Co^{2+}$ . The shape and the large half-width of the peak presuppose also the presence of small amounts of  $Co^{3+}$  and  $Co^0$ .

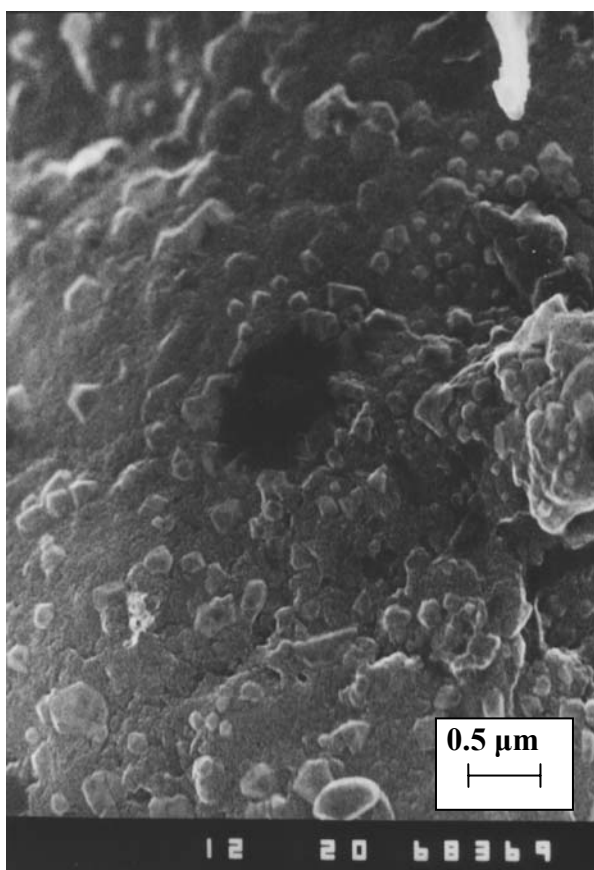


Fig. 4. SEM microphotograph of the Co oxide layer ( $\times 20000$ ).

The systematic studies performed on the possibility of electrochemical preparation of  $ZrO_2$ - $CeO_2$ - $YO_{1.5}$  layers showed this method to be suitable for varying the Ce/Zr ratio over a wide range (0.5–11) at a constant concentration of yttria. It was also established that a subsequent electrochemical deposition of certain amounts of CoO on these layers was possible. In the present paper we

concentrated on systems characterized by the formula  $[(CeO_2)_{70.8}(ZrO_2)_{9.2}(YO_{1.5})_{20.0}]/Ni$ ,  $Co_{34.4}[(CeO_2)_{46.4}(ZrO_2)_{6.0}(YO_{1.5})_{13.1}]/Ni$  and  $Co_{36.5}[(CeO_2)_{45.0}(ZrO_2)_{5.8}(YO_{1.5})_{12.7}]/Ni$ .

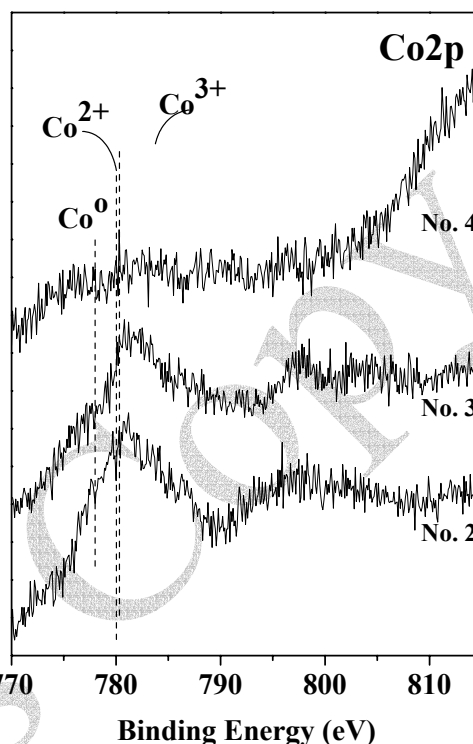


Fig. 5. XPS spectra originated by  $Co^0$ ,  $Co^{2+}$  and  $Co^{3+}$   
 (No. 2 –  $Co_{36.5}[(CeO_2)_{45.0}(ZrO_2)_{5.8}(YO_{1.5})_{12.7}]/Ni$ ;  
 No. 3 –  $Co_{34.4}[(CeO_2)_{46.4}(ZrO_2)_{6.0}(YO_{1.5})_{13.1}]/Ni$ ;  
 No. 4 –  $[(CeO_2)_{70.8}(ZrO_2)_{9.2}(YO_{1.5})_{20.0}]/Ni$ ).

#### Electrocatalytic investigations

Results from preliminary electrocatalytic studies are presented in Figs. 6–8. The curves characterize the electrodes behavior as follows: 1 - Ni substrate; 4 - Ni substrate with a ceria-zirconia-yttria layer deposited on it (electrode No. 4 -  $[(CeO_2)_{70.8}(ZrO_2)_{9.2}(YO_{1.5})_{20.0}]/Ni$ ); 2 and 3 - the system  $(CeO_2)_{70.8}(ZrO_2)_{9.2}(YO_{1.5})_{20.0}/Ni$  on which a Co oxide film with two different concentrations has been additionally deposited (electrodes Nos. 2 and 3).

The anodic polarization curves (Fig. 6) show that the Ce-Zr-Y system itself has no favorable effect on the kinetics of oxygen evolution (electrode No. 4). Its combination with additionally deposited Co oxide showed a positive effect. Better catalytic properties were demonstrated by electrode No. 2 ( $Co_{36.5}[(CeO_2)_{45.0}(ZrO_2)_{5.8}(YO_{1.5})_{12.7}]/Ni$ ), characterized by an  $E_A$  value lower than that in the case of pure Ni electrode by about 150 mV. This electrode is comparable with the best electrodes obtained by vacuum evaporation [28]: when  $I = 50 \text{ mA/cm}^2$ ,  $E_A$  is about +750 mV (Hg/HgO). The Tafel curves also

confirm this conclusion (Fig. 7). It should be noted that the conditions of obtaining these curves ( $i < 1 \text{ mA/cm}^2$ ) are the optimum ones for the electrodes to demonstrate their catalytic properties since it is known that with such current densities there are no diffusion and other hindrances characteristic of higher current charges and the rate of oxygen evolution only depends on kinetic restrictions characterizing the catalytic properties of the systems under consideration.

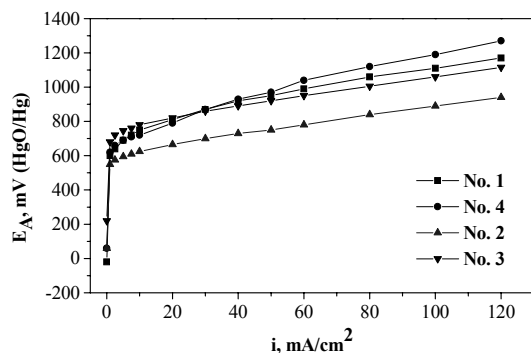


Fig. 6. Anodic polarization curves of investigated electrodes in the plot  $i-E_A$ .

At this stage of studies the effect of the amount of deposited CoO on the electrocatalytic properties of the system  $\text{CoO}/\text{CeO}_2\text{-ZrO}_2\text{-Y}_2\text{O}_3/\text{Ni}$  cannot be determined due to the small difference in the amounts of electrodeposited cobalt oxide (6.3 and 6.9 at.%, which is within error limits). The great difference found between the electrochemical activities of the two Co/Zr-Ce-Y/Ni electrodes (curves 2 and 3 in Fig. 6) is, according to us, most probably due to a difference in dispersion of the deposited CoO, a problem which is to be studied in the future.

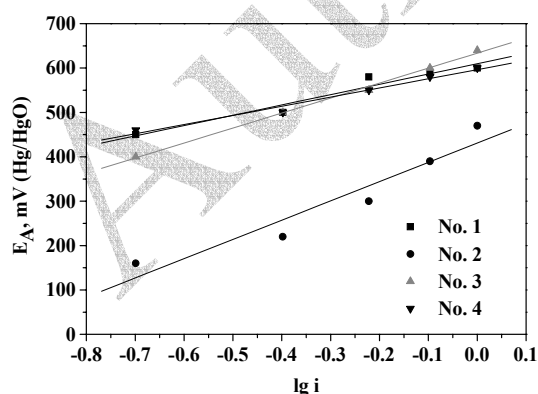


Fig. 7. Anodic polarization curves of investigated electrodes in the plot  $\lg i-E_A$ .

The polarization cathode curves show that at introducing oxygen to the oxide layers of GDE (Fig. 8), all electrodes have practically the same

characteristics. With respect to oxygen reduction they reach relatively low densities of cathode current (30–40  $\text{mA/cm}^2$ ). At higher values they are obviously inappropriate since the cathode potential reaches values smaller than  $-500 \text{ mV}$  where irreversible processes with Co oxides can set in. This is, according to us, due to insufficient optimization of GDE with respect to oxygen diffusion.

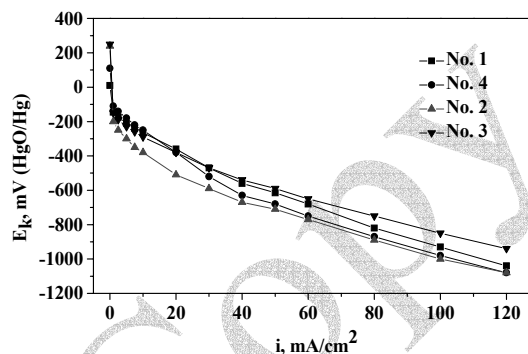


Fig. 8. Cathodic polarization curves of investigated electrodes in the plot  $i-E_K$ .

## CONCLUSIONS

The results obtained show that the electrochemical method of obtaining layers of mixed ceria, zirconia and yttria on various metal substrates permits controlled formation of ternary oxide systems with defined compositions. Varying the ion concentration of Ce, Zr and Y in the electrolyte and the electric regime of deposition one may change the quantitative ratio of the components over wide ranges. In addition, domination of the reduction of cerium ions over the deposition was found, the ions being reduced on active substrate parts, this determining mainly “island” deposition of ceria while the distribution of the zirconium and yttrium-containing components is uniform. This way of deposition forms zones with different concentrations of cerium on the layer surface and non-uniform cracks. The X-ray studies indicate incorporation of zirconium and yttrium into the cubic lattice of cerium and formation of a solid solution, no separate phases of ceria, zirconia and yttria being observed. SEM and EDS analyses evidence a fine dispersion and crystallite sizes of the order of 200 nm.

Electrocatalytic tests showed that the investigated ternary oxide system does not display catalytic effect on the evolution of oxygen and hydrogen in alkaline media. However, combined with additionally electrodeposited CoO, it demonstrates a very favourable influence on the evolution of oxygen, reducing the reaction potential by about 200 mV.

REFERENCES

1. P. Fornasiero, J. Kaspar, V. Sergo, M. Graziani, *J. Catal.*, **182**, 56 (1999).
2. S. J. Schmiege, D. N. Belton, *Appl. Catal. B.: Environ.*, **6**, 127 (1995).
3. P. Vidmar, P. Fornasiero, J. Kaspar, G. Gubitosa, M. Graziani, *J. Catal.*, **171**, 160 (1997).
4. K. Minami, T. Masui, N. Imanaka, L. Dai, B. Pacaud, *J. Alloy Compd.*, **408–412**, 1132 (2006).
5. P. Vidmar, P. Fornasiero, J. Kaspar, G. Gubitosa, M. Graziani, *J. Catal.*, **171**, 160 (1997).
6. C. Lopez-Cartes, J. A. Perez-Omil, J. M. Pintado, J. J. Calvino, Z. C. Kang, L. Eyring, *Ultramicroscopy*, **80**, 19 (1999)
7. J. C. Vargas, S. Libs, A.-C. Roger, A. Kiennemann, *Catal. Today*, **107–108**, 417 (2005).
8. N. Laosiripojana, S. Assabumrungrat, *Appl. Catal. A: Gen.*, **290**, 200 (2005).
9. S. J. Schneider, T. Negas, H. P. R. Frederikse, *Rev. Int. Hautes Temp. Refract.*, **16**, 669 (1979).
10. S. F. Palguez, Z. S. Volchenkova, *Zh. Phys. Khim. SSSR*, **34**, 211 (1960).
11. F. F. Lange, *Rockwell Int. Tech. Rept.*, 12 (1981) ONR-N00014-77-C-0441
12. N. Sakai, T. Hashimoto, T. Katsube, K. Yamaji, H. Negishi, T. Horita, H. Yokokawa, Y. P. Xiong, M. Nakagawa, Y. Takahashi, *Solid State Ionics*, **143**, 151 (2001).
13. J.-H. Lee, J. Kim, S.-W. Kim, H.-W. Lee, H. S. Song, *Solid State Ionics*, **166**, 45 (2004).
14. K. Minami, T. Masui, N. Imanaka, L. Dai, B. Pacaud, *J. Alloy Compd.*, **408–412**, 1132 (2006).
15. Z. C. Kang, L. Eyring, *J. Solid State Chem.*, **155**, 129 (2000).
16. Y. Xiong, K. Yamaji, N. Sakai, H. Negishi, T. Horita, H. Yokokawa, *J. Electrochem. Soc.*, **148**, E489 (2001).
17. I. Avramova, D. Stoychev, Ts. Marinova, *Appl. Surf. Sci.*, **253**, 1365 (2006).
18. Ts. Marinova, A. Tsanev, D. Stoychev, *Mater. Sci. Eng: B*, **130**, 1 (2006).
19. J. Kaspar, P. Fornasiero, G. Balducci, R. Di Monte, N. Hickey, V. Sergo, *Inorg. Chim. Acta*, **349**, 217 (2003).
20. A. M. Ginberg, *Galvanotekhnika (Handbook), Metallurgia, Moscow*, 1987, p. 87 (in Russian).
21. J. H. Scofield, *J. Electron. Spectrosc. Relat. Phenom.*, **8**, 129 (1976).
22. S. Bedrane, C. Descorme, D. Duprez, *Catal. Today*, **75**, 401 (2002).
23. M. Yashima, H. Arashi, M. Kakihana, M. Yoshimura, *J. Am. Ceram. Soc.*, **77**, 1067 (1994).
24. C. E. Hori, H. Permana, K. Y. Simon Ng, A. Brenner, K. More, K. M. Rahmoeller, D. Belton, *Appl. Catal. B: Environ.*, **16**, 105 (1998).
25. A. Cabanas, J. A. Darr, E. Lester, M. Poliakoff, *Chem. Commun.*, **11**, 901 (2000).
26. Y. Xiong, K. Yamaji, N. Sakai, H. Negishi, T. Horita, H. Yokokawa, *J. Electrochem. Soc.*, **148**, E489 (2001).
27. V. Rashkova, PhD Thesis, Centr. Lab. Photoprocesses, Bulg. Acad. Sci., Sofia, 2007.

ЕЛЕКТРОКАТАЛИТИЧНА АКТИВНОСТ НА ЕЛЕКТРОХИМИЧНО ОТЛОЖЕНИ Zr-Ce-Y/Ni И Co/Zr-Ce-Y/Ni ОКСИДНИ СИСТЕМИ ПРИ ОТДЕЛЯНЕТО НА ВОДОРОД И КИСЛОРОД

Ал. С. Цанев<sup>1</sup>, П. Ц. Илиев<sup>2</sup>, К. М. Петров<sup>2</sup>, П. К. Стефанов<sup>1</sup>, Д. С. Стойчев<sup>3\*</sup>

<sup>1</sup> Институт по обща и неорганична химия, Българска академия на науките, ул. „Акад. Г. Бончев“, бл. 11, 1113 София

<sup>2</sup> Институт по електрохимия и енергийни системи, Българска академия на науките, ул. „Акад. Г. Бончев“, бл. 10, 1113 София

<sup>3</sup> Институт по физикохимия „Акад. Р. Кашиев“, Българска академия на науките, ул. „Акад. Г. Бончев“, бл. 10, 1113 София

Постъпила на 28 януари 2008 г., Преработена на 25 февруари 2008 г.

(Резюме)

Изследвана е възможността за електрохимично получаване на смесени оксиди от CeO<sub>2</sub>-ZrO<sub>2</sub>-Y<sub>2</sub>O<sub>3</sub> върху Ni-пяна. Върху така формираните тънки слоеве е електроотложен кобалтов оксид. Изучено е каталитичното поведение на така получената система по отношение на реакциите на отделяне на водород и кислород в алкални електролити. Изследвано е влиянието на условията на електроотлагане върху съотношението на трите компонента Ce:Zr:Y във формираните слоеве. Дефинирани са структурата, морфологията и разпределението на елементите. Показано е, че системата CoO/CeO<sub>2</sub>-ZrO<sub>2</sub>-Y<sub>2</sub>O<sub>3</sub>/Ni катализира реакцията на отделяне на кислород, измествайки потенциала и с около 200 mV в положителна посока.